# Expanded View Figures

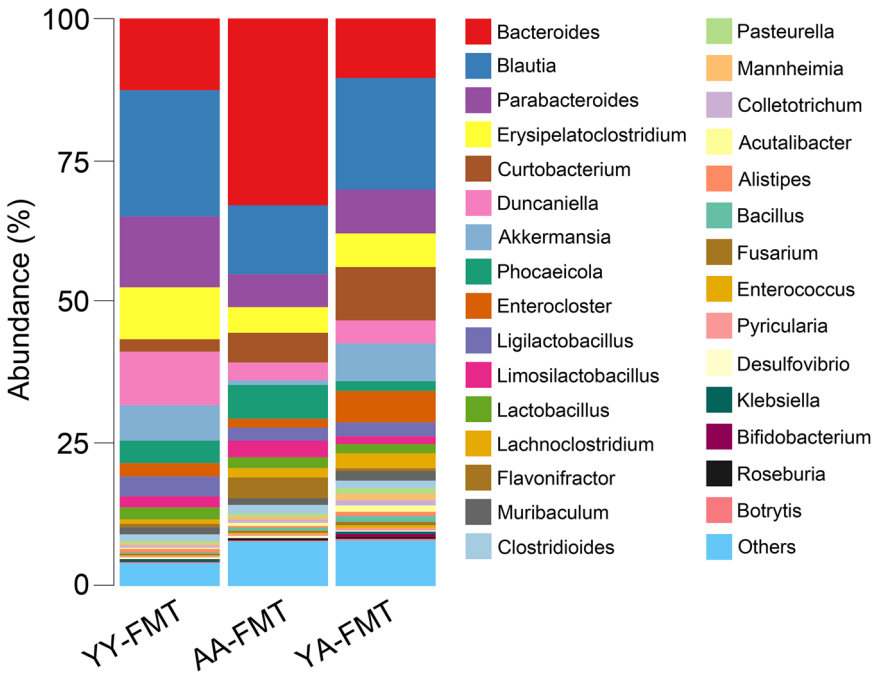


**Figure EV1. Effects of FMT on the bacterial abundance in mice.**

The degree of bacterial taxonomic similarity of gut microbiota was analyzed in YY-FMT, AA-FMT, and YA-FMT groups at genus level.

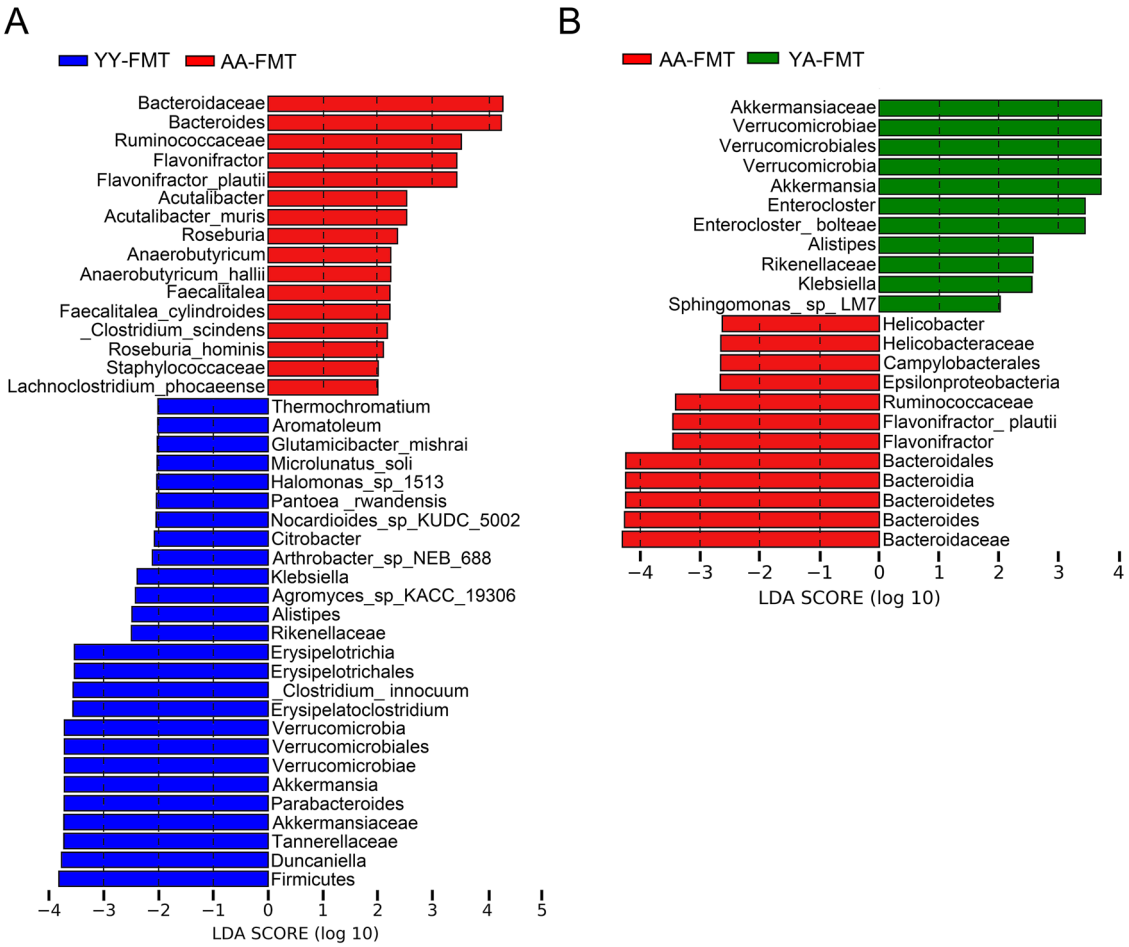


**Figure EV2. Effects of FMT on the bacterial taxa in mice.**

(**A**) LEfSe showed dominant bacterial taxa in AA-FMT group compared to YY-FMT group. Blue bar represented YY-FMT, and red bar represented AA-FMT. (**B**) LEfSe showed dominant bacterial taxa in YA-FMT group compared to AA-FMT group. Red bar represented AA-FMT, and green bar represented YA-FMT.

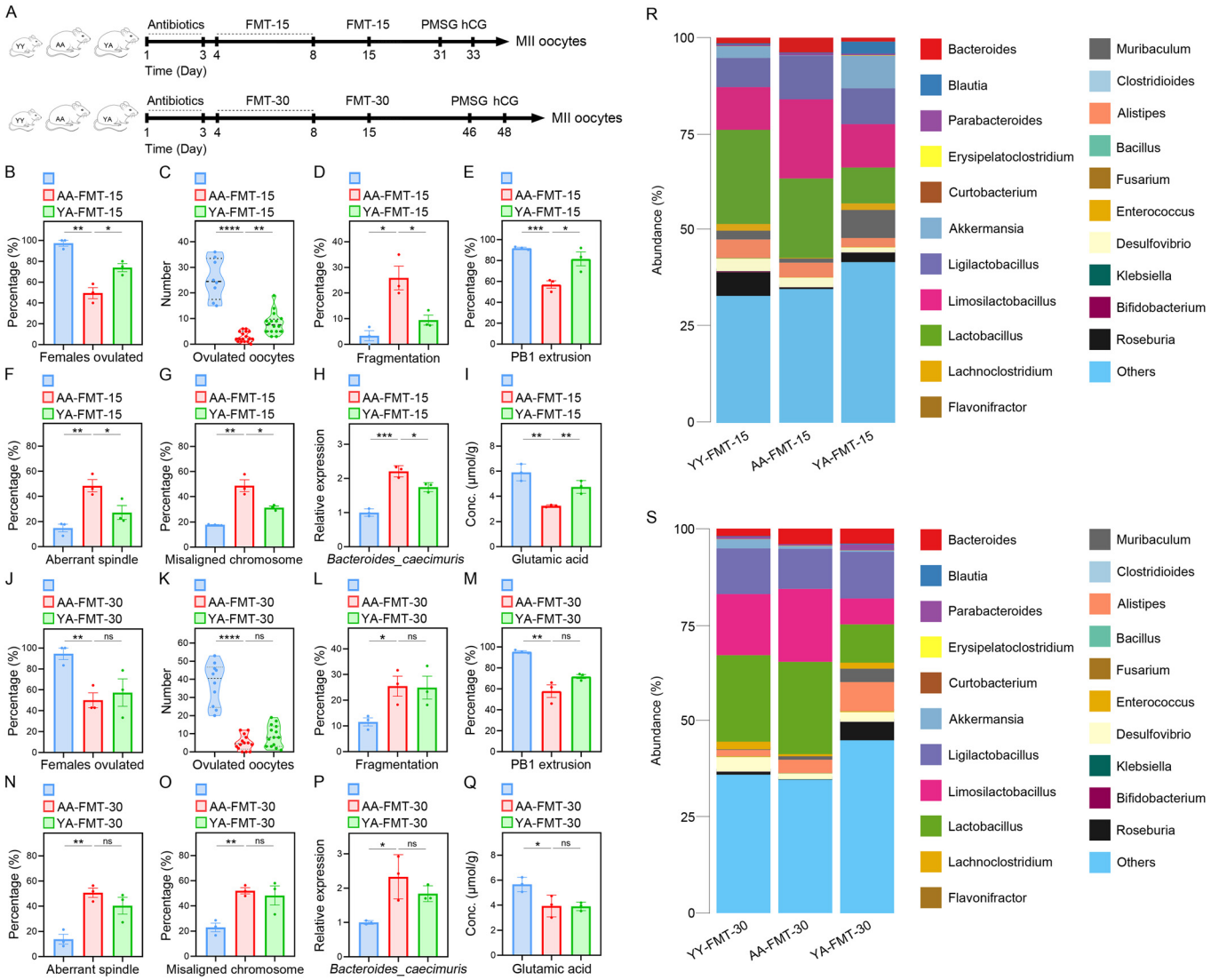


**Figure EV3. Effects of young gut microbiota on the quality of aged oocytes on days 15 and 30 after FMT.**

(**A**) A timeline scheme for antibiotics treatment, FMT, hormone injection and subsequent analyses. (**B**) The percentage of female mice that were ovulated in YY-FMT-15 ($n = 30$), AA-FMT-15 ($n = 36$), and YA-FMT-15 ($n = 38$) group. $^{**}P = 0.0013$, $^{*}P = 0.0205$. (**C**) The number of ovulated oocytes was counted in YY-FMT-15 ($n = 8$), AA-FMT-15 ($n = 17$), and YA-FMT-15 ($n = 16$) mice. $^{****}P < 0.0001$, $^{**}P = 0.0032$. (**D**) The proportion of fragmented oocytes was quantified in YY-FMT-15 ($n = 112$), AA-FMT-15 ($n = 67$), and YA-FMT-15 ($n = 96$) mice. $^{*}P = 0.0109$, $^{*}P = 0.0303$. (**E**) The rate of PB1 extrusion was quantified in YY-FMT-15 ($n = 112$), AA-FMT-15 ($n = 67$), and YA-FMT-15 ($n = 96$) oocytes. $^{**}P = 0.0007$, $^{*}P = 0.0312$. (**F**) The rate of aberrant spindles was quantified in YY-FMT-15 ($n = 73$), AA-FMT-15 ($n = 110$), and YA-FMT-15 ($n = 67$) oocytes at MII stage. $^{**}P = 0.0044$, $^{*}P = 0.0445$. (**G**) The rate of misaligned chromosomes was quantified in YY-FMT-15 ($n = 73$), AA-FMT-15 ($n = 110$), and YA-FMT-15 oocytes ($n = 67$) at M II stage. $^{**}P = 0.0029$, $^{*}P = 0.0241$. (**H**) The abundance of *Bacteroides_caecimuris* was determined by qPCR in YY-FMT-15, AA-FMT-15, and YA-FMT-15 mice. $^{***}P = 0.0005$, $^{*}P = 0.0186$. (**I**) Glutamic acid levels were quantified in YY-FMT-15 ($n = 21$), AA-FMT-15 ($n = 16$), and YA-FMT-15 ($n = 15$) ovaries. $^{**}P = 0.0073$, $^{**}P = 0.0024$. (**J**) The percentage of female mice that were ovulated in YY-FMT-30 ($n = 32$), AA-FMT-30 ($n = 42$), and YA-FMT-30 ($n = 36$) group. $^{**}P = 0.0080$, $P = 0.6508$. (**K**) The number of ovulated oocytes was counted in YY-FMT-30 ($n = 10$), AA-FMT-30 ($n = 14$), and YA-FMT-30 ($n = 14$) mice. $^{****}P < 0.0001$, $P = 0.0604$. (**L**) The proportion of fragmented oocytes was quantified in YY-FMT-30 ($n = 492$), AA-FMT-30 ($n = 217$), and YA-FMT-30 ($n = 151$) mice. $^{*}P = 0.0299$, $P = 0.9346$. (**M**) The rate of PB1 extrusion was quantified in YY-FMT-30 ($n = 492$), AA-FMT-30 ($n = 217$), and YA-FMT-30 ($n = 151$) oocytes. $^{**}P = 0.0035$, $P = 0.0931$. (**N**) The rate of aberrant spindles was quantified in YY-FMT-30 ($n = 98$), AA-FMT-30 ($n = 114$), and YA-FMT-30 ($n = 107$) oocytes at M II stage. $^{**}P = 0.0024$, $P = 0.2500$. (**O**) The rate of misaligned chromosomes was quantified in YY-FMT-30 ($n = 98$), AA-FMT-30 ($n = 114$), and YA-FMT-30 oocytes ($n = 107$) at MII stage. $^{**}P = 0.0023$, $P = 0.6616$. (**P**) The abundance of *Bacteroides_caecimuris* was determined by qPCR in YY-FMT-30, AA-FMT-30, and YA-FMT-30 mice. $^{*}P = 0.0235$, $P = 0.2804$. (**Q**) Glutamic acid levels were quantified in YY-FMT-30 ($n = 22$), AA-FMT-30 ($n = 16$), and YA-FMT-30 ($n = 16$) ovaries. $^{**}P = 0.0453$, $P = 0.9562$. (**R**) The degree of bacterial taxonomic similarity of gut microbiota was analyzed in YY-FMT-15, AA-FMT-15, and YA-FMT-15 groups at genus level. (**S**) The degree of bacterial taxonomic similarity of gut microbiota was analyzed in YY-FMT-30, AA-FMT-30, and YA-FMT-30 groups at genus level. Data in (**B–Q**) were presented as mean ± SEM or SD of at least three independent experiments. $^{*}P < 0.05$; $^{**}P < 0.01$; $^{***}P < 0.001$; $^{****}P < 0.0001$; ns, no significance. Statistical significance was determined by two-tailed unpaired t-test.

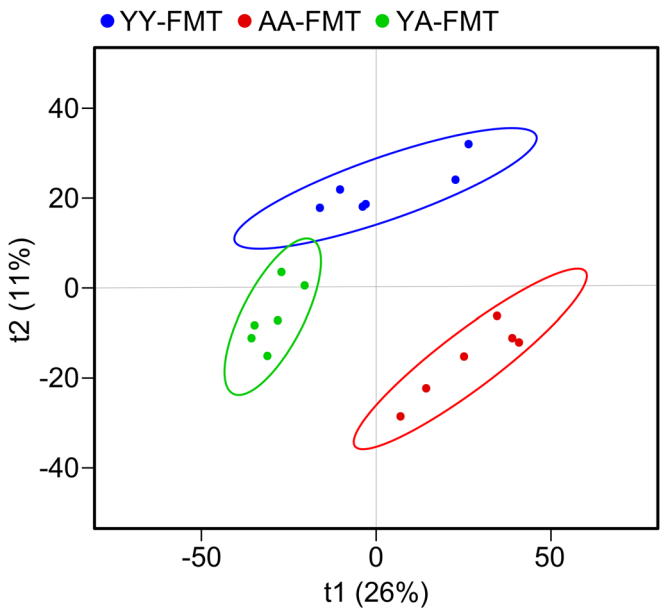


**Figure EV4. PLS-DA plot showing the metabolome samples from FMT mice.**

Blue circles represented samples from YY-FMT group, red circles represented samples from AA-FMT group, and green circles represented samples from YA-FMT group.

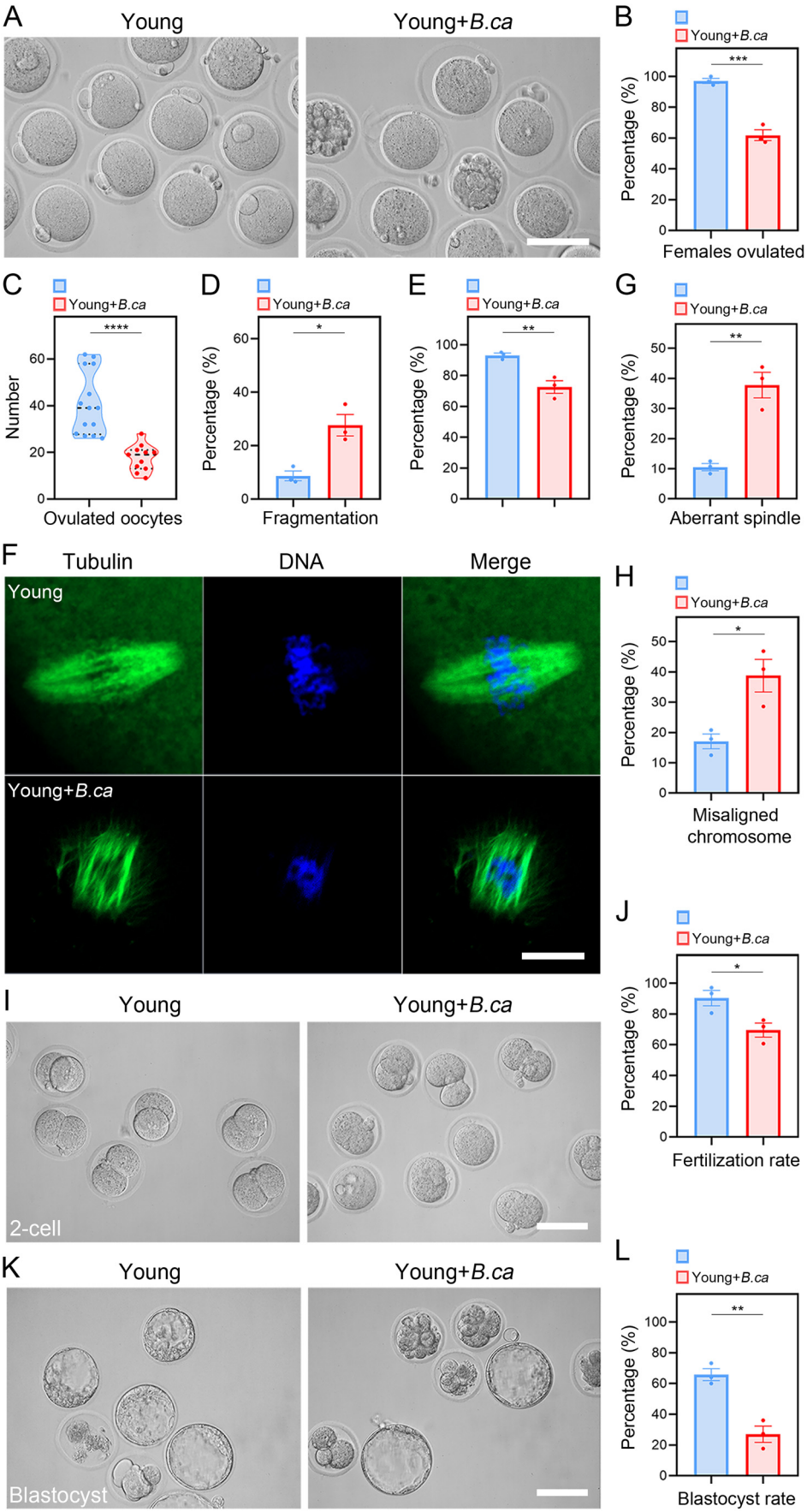
A
Young
Young+B.ca
B
Young+B.ca
***
Percentage (%)
Females ovulated
C
Young+B.ca
****
Number
Ovulated oocytes
D
Young+B.ca
*
Percentage (%)
Fragmentation
E
Young+B.ca
**
Percentage (%)
G
Young+B.ca
**
Percentage (%)
Aberrant spindle
F
Tubulin
DNA
Merge
Young
Young+B.ca
H
Young+B.ca
*
Percentage (%)
Misaligned chromosome
J
Young+B.ca
*
Percentage (%)
Fertilization rate
I
Young
Young+B.ca
2-cell
K
Young
Young+B.ca
Blastocyst
L
Young+B.ca
**
Percentage (%)
Blastocyst rate

**Figure EV5. Effects of *Bacteroides_caecimuris* supplementation in young mice on the oocyte quality.**

(**A**) Representative images of ovulated oocytes collected from young and young+*B.ca* mice. Scale bar, 80 μm. (**B**) The percentage of female mice that were ovulated in young ($n = 86$) and young+*B.ca* ($n = 118$) group. ***$P = 0.0008$. (**C**) The number of ovulated oocytes was counted in young ($n = 14$) and young+*B.ca* ($n = 11$) mice. ****$P < 0.0001$. (**D**) The proportion of fragmented oocytes was quantified in young ($n = 575$) and young+*B.ca* ($n = 194$) mice. *$P = 0.0126$. (**E**) The rate of PB1 extrusion was quantified in young ($n = 575$) and young+*B.ca* ($n = 194$) oocytes. **$P = 0.0087$. (**F**) Representative images of the spindle morphology and chromosome alignment in young and young+*B.ca* oocytes at M II stage. Scale bar, 20 μm. (**G**) The rate of aberrant spindles was quantified in young ($n = 76$) and young+*B.ca* ($n = 111$) oocytes at M II stage. **$P = 0.0035$. (**H**) The rate of misaligned chromosomes was quantified in young ($n = 76$) and young+*B.ca* ($n = 111$) at M II stage. *$P = 0.0213$. (**I**) Representative images of 2-cell embryos in young and young+*B.ca* groups. Scale bar, 80 μm. (**J**) The fertilization rate was quantified in young ($n = 101$) and young+*B.ca* ($n = 85$) groups. *$P = 0.0373$. (**K**) Representative images of blastocysts in young and young+*B.ca* groups. Scale bar, 80 μm. (**L**) The blastocyst formation rate was quantified in young ($n = 115$) and young+*B.ca* ($n = 84$) groups. **$P = 0.0041$. Data in (**B**), (**C**), (**D**), (**E**), (**G**), (**H**), (**J**), and (**L**) were presented as mean ± SEM or SD of at least three independent experiments. *$P < 0.05$; **$P < 0.01$; ***$P < 0.001$; ****$P < 0.0001$. Statistical significance was determined by two-tailed unpaired t-test.

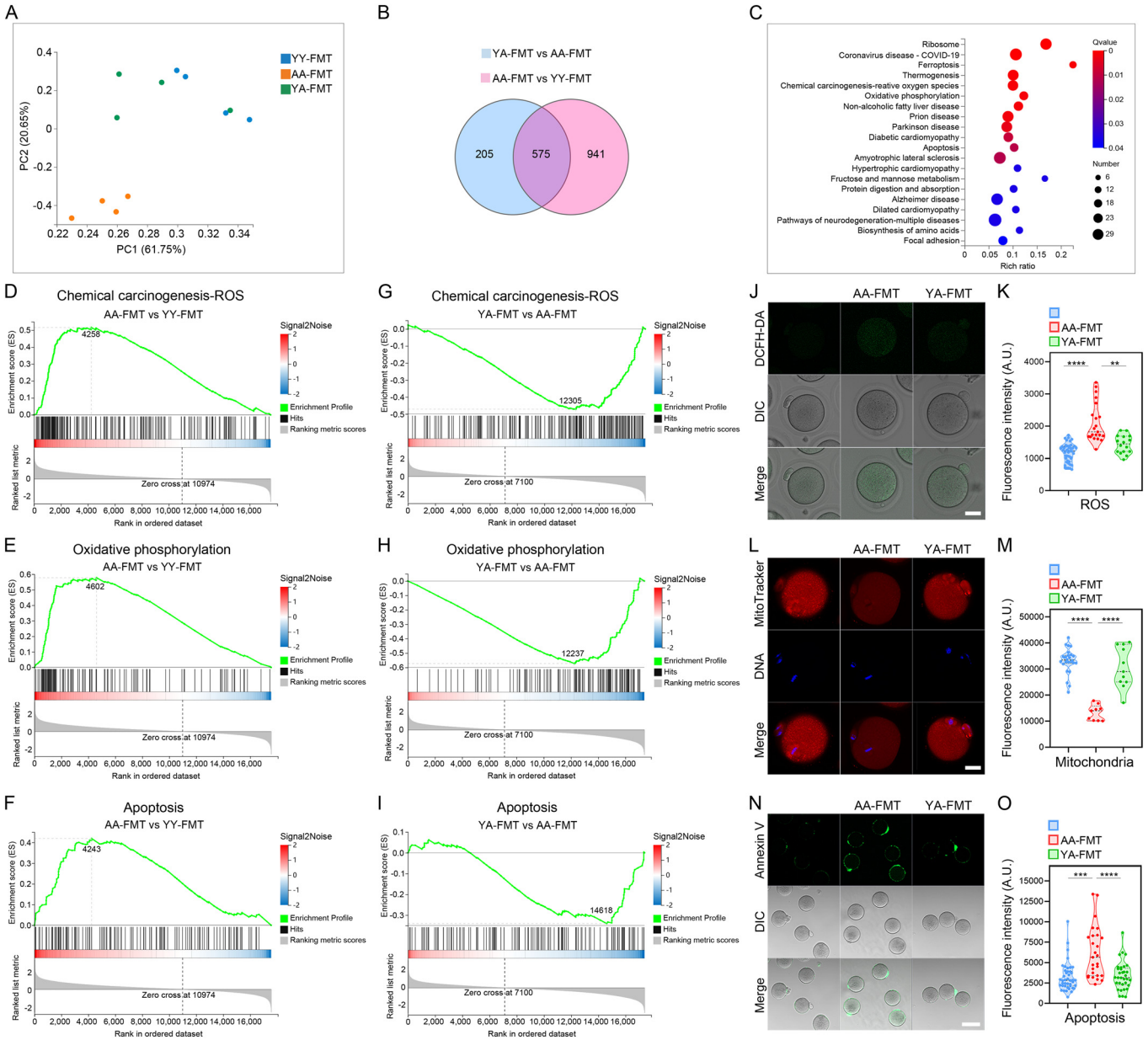


**Figure EV6. Supplementary transcriptome data related to Fig. 5.**

(**A**) PCA plot displayed the oocyte samples from YY-FMT, AA-FMT, and YA-FMT mice. Blue circles represented samples from YY-FMT group, orange circles represented samples from AA-FMT group, and green circles represented samples from YA-FMT group. (**B**) Venn diagram showed the number of overlapping differential transcripts between AA-FMT compared to YY-FMT group and YA-FMT compared to AA-FMT group. (**C**) KEGG enrichment analysis of overlapping differential transcripts between AA-FMT compared to YY-FMT group and YA-FMT compared to AA-FMT group. (**D**) GSEA plot showed genes involved in the ROS pathway (AA-FMT positively correlated; YY-FMT negatively correlated). (**E**) GSEA plot showed genes involved in the oxidative phosphorylation pathway (AA-FMT positively correlated; YY-FMT negatively correlated). (**F**) GSEA plot showed genes involved in the apoptosis pathway (AA-FMT positively correlated; YY-FMT negatively correlated). (**G**) GSEA plot showed genes involved in the ROS pathway (YA-FMT positively correlated; AA-FMT negatively correlated). (**H**) GSEA plot showed genes involved in the oxidative phosphorylation pathway (YA-FMT positively correlated; AA-FMT negatively correlated). (**I**) GSEA plot showed genes involved in the apoptosis pathway (YA-FMT positively correlated; AA-FMT negatively correlated). (**J**) Representative images of ROS levels as detected by DCFH-DA staining in YY-FMT, AA-FMT, and YA-FMT oocytes. Scale bar, 20 μm. (**K**) The fluorescence intensity of ROS signals was quantified in YY-FMT ($n = 45$), AA-FMT ($n = 21$), and YA-FMT ($n = 16$) oocytes. $^{****}P < 0.0001$, $^{**}P = 0.0034$. (**L**) Representative images of mitochondria as stained with MitoTracker Red in YY-FMT, AA-FMT, and YA-FMT oocytes. Scale bar, 20 μm. (**M**) The fluorescence intensity of mitochondrial signals was measured in YY-FMT ($n = 26$), AA-FMT ($n = 9$), and YA-FMT ($n = 11$) oocytes. $^{****}P < 0.0001$, $^{****}P < 0.0001$. (**N**) Representative images of apoptotic oocytes as stained with Annexin-V in YY-FMT, AA-FMT, and YA-FMT groups. Scale bar, 80 μm. (**O**) The fluorescence intensity of Annexin-V signals on the membrane was quantified in YY-FMT ($n = 42$), AA-FMT ($n = 27$), and YA-FMT ($n = 33$) oocytes. $^{***}P = 0.0003$, $^{****}P < 0.0001$. Data in (**K**), (**M**), and (**O**) were presented as mean ± SD of at least three independent experiments. $^{**}P < 0.01$; $^{***}P < 0.001$; $^{****}P < 0.0001$. Statistical significance was determined by two-tailed unpaired t-test.

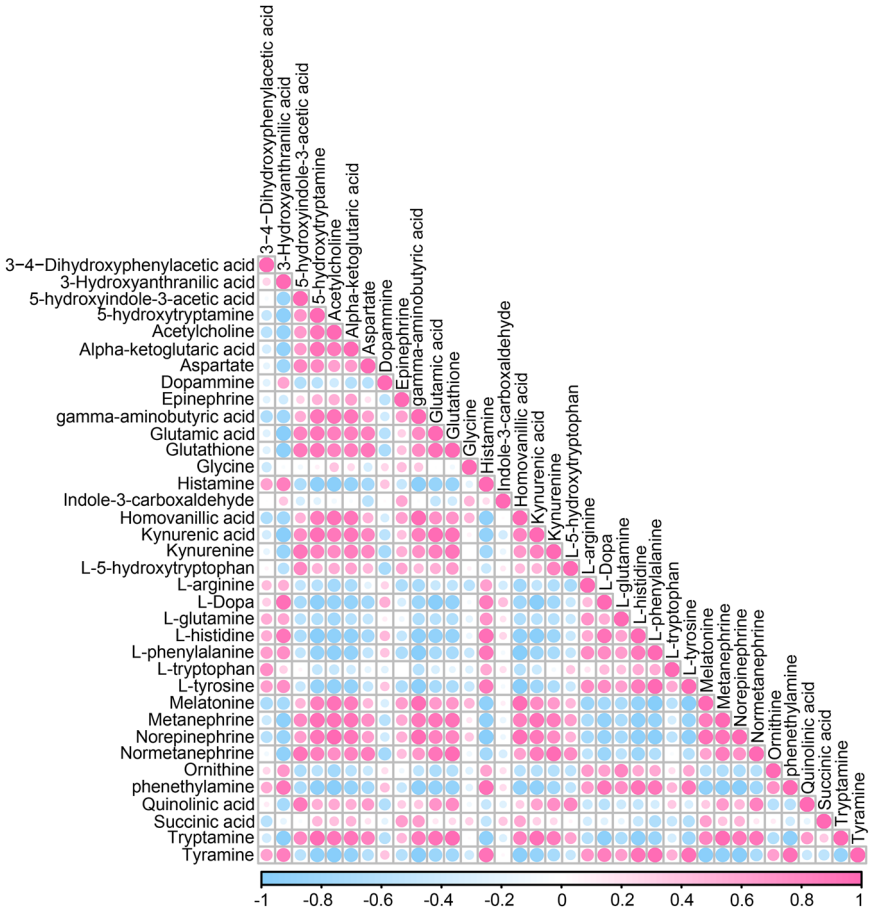


**Figure EV7. Spearman's correlation analysis of neurotransmitter metabolites.**

Red represented positive correlation, and blue represented negative correlation. The darker the color, the stronger the correlation.

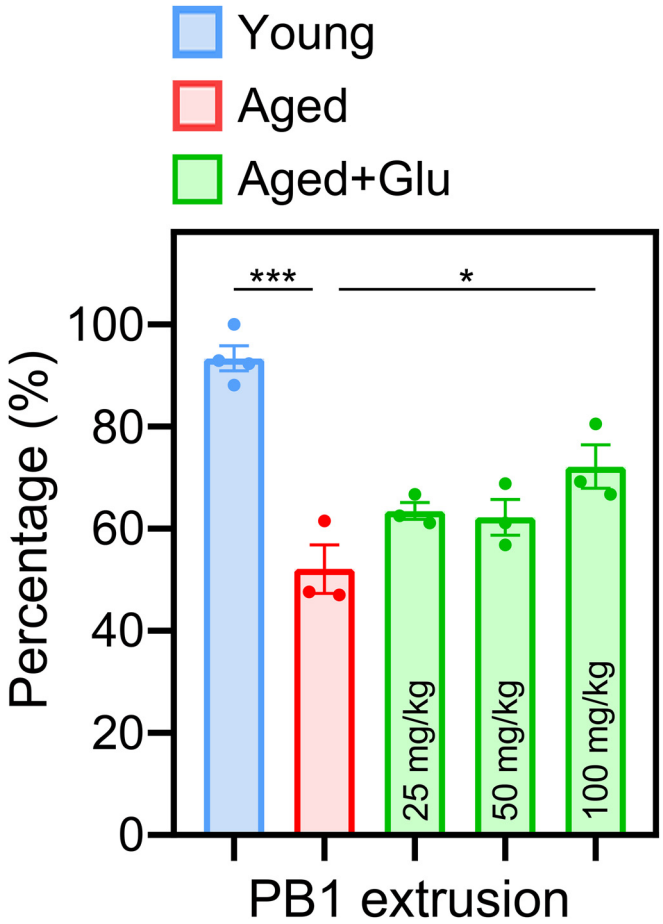


**Figure EV8. Effects of different concentrations of glutamic acid on the maturation of aged oocytes.**

The percentage of PB1 extrusion was quantified in young ($n = 222$), aged ($n = 51$), and aged+Glu (25 mg/kg: $n = 38$, 50 mg/kg: $n = 71$, 100 mg/kg: $n = 88$) oocytes. ***$P = 0.0004$, *$P = 0.0344$. Data were presented as mean ± SEM of at least three independent experiments. *$P < 0.05$; ***$P < 0.001$. Statistical significance was determined by two-tailed unpaired t-test.

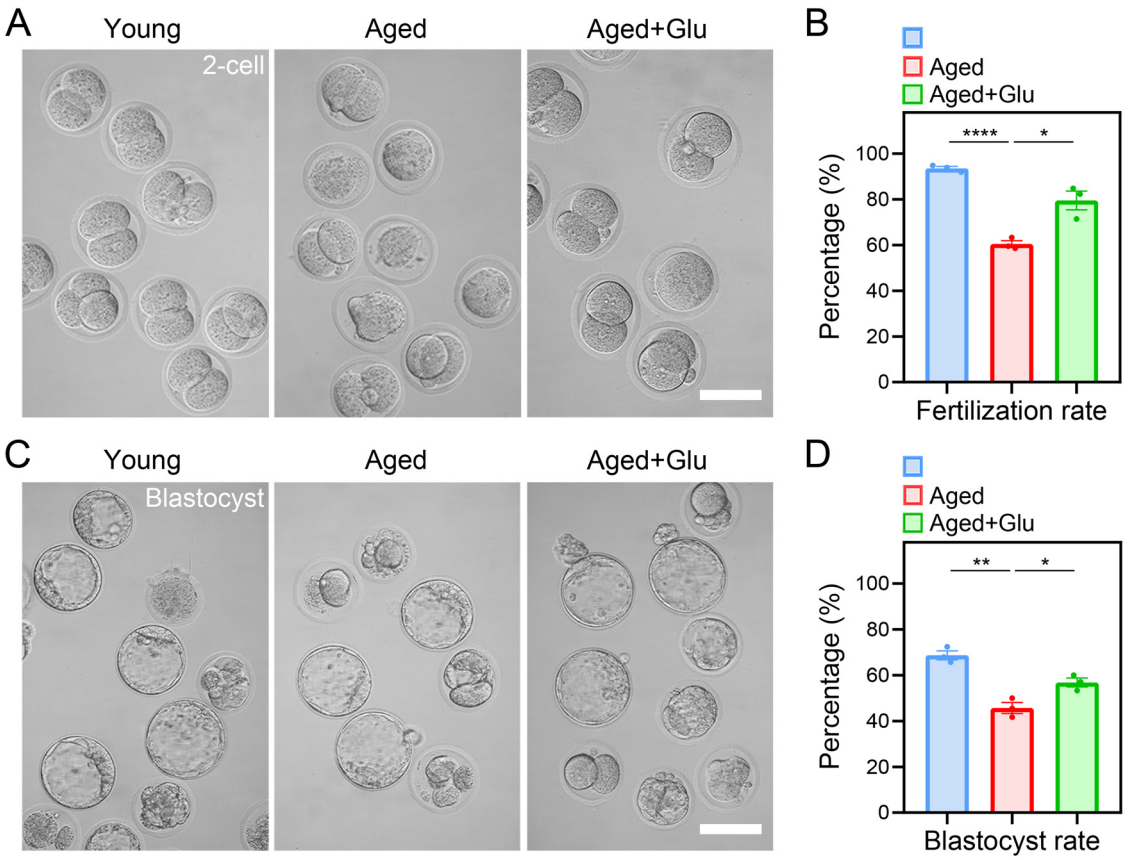


**Figure EV9. Effects of glutamic acid supplementation on the fertilization and early embryonic development in aged mice.**

(**A**) Representative images of 2-cell embryos in young, aged, and aged+Glu groups. Scale bar, 80 μm. (**B**) The fertilization rate was quantified in young ($n = 128$), aged ($n = 96$), and aged+Glu ($n = 78$) groups. ****$P < 0.0001$, *$P = 0.0120$. (**C**) Representative images of blastocysts in young, aged, and aged+Glu groups. Scale bar, 80 μm. (**D**) The blastocyst formation rate was quantified in young ($n = 143$), aged ($n = 58$), and aged+Glu ($n = 48$) groups. **$P = 0.0018$, *$P = 0.0227$. Data in (**B**) and (**D**) were presented as mean ± SEM of at least three independent experiments. *$P < 0.05$; **$P < 0.01$; ****$P < 0.0001$. Statistical significance was determined by two-tailed unpaired t-test.

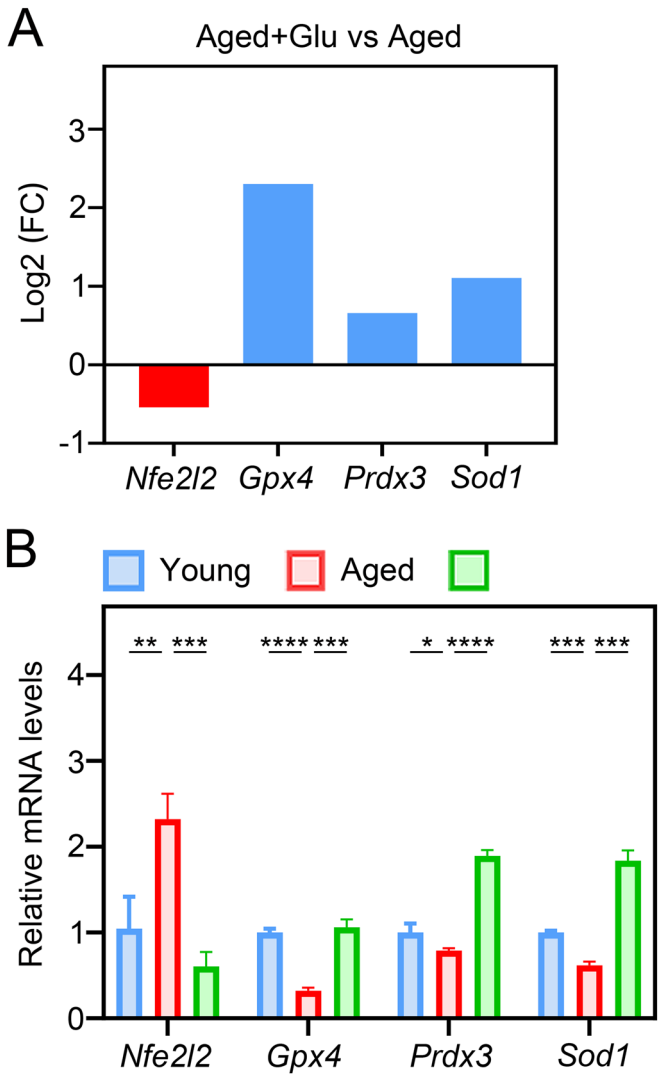


**Figure EV10. Effects of glutamic acid supplementation on the transcript levels of some antioxidant genes.**

(**A**) RNA-seq results of selected antioxidant genes in aged+Glu oocytes compared to aged ones. (**B**) Validation of RNA-seq data by quantitative RT-PCR in young ($n = 60$), aged ($n = 60$), and aged+Glu ($n = 60$) oocytes. $^{**}P = 0.0065$, $^{***}P = 0.0009$, $^{****}P < 0.0001$, $^{***}P = 0.0002$, $^{*}P = 0.0131$, $^{****}P < 0.0001$, $^{***}P = 0.0002$, $^{***}P = 0.0002$. Data in (**B**) were presented as mean ± SEM of at least three independent experiments. $^{*}P < 0.05$; $^{**}P < 0.01$; $^{***}P < 0.001$; $^{****}P < 0.0001$. Statistical significance was determined by multiple t-test.

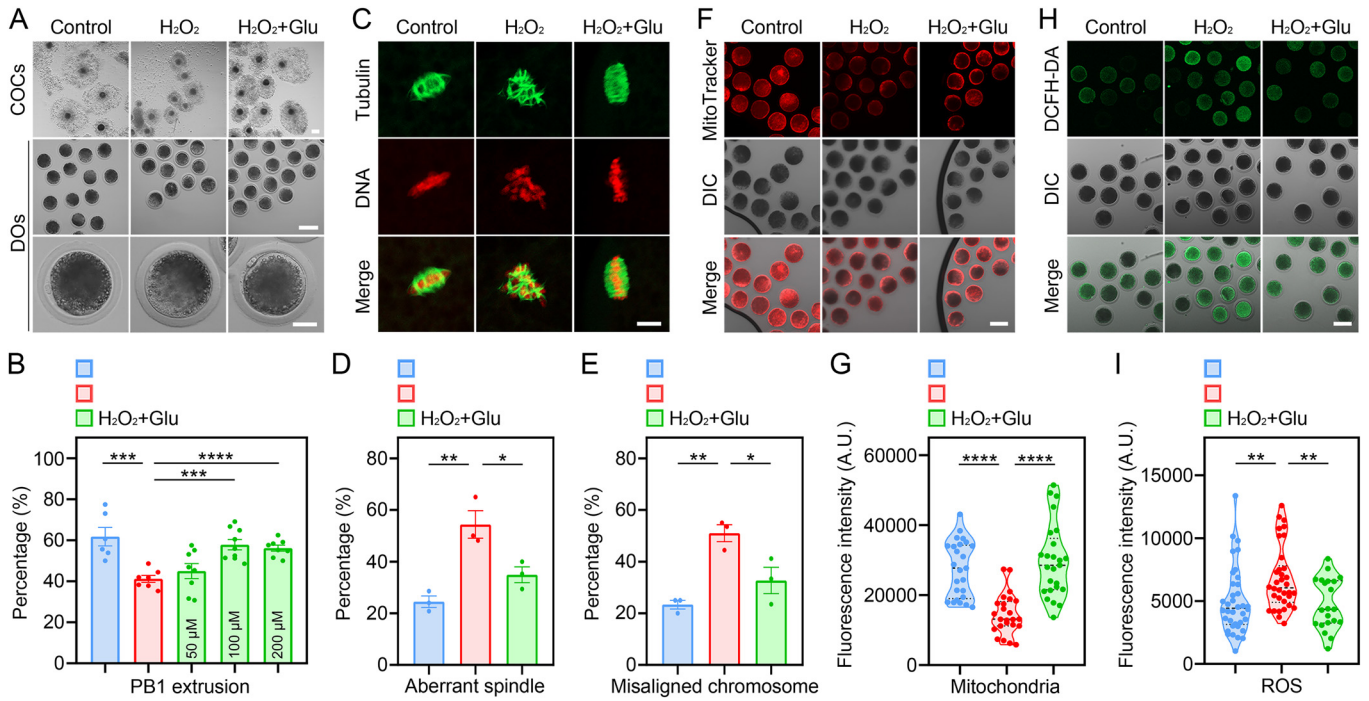


**Figure EV11. Effects of glutamic acid supplementation on the quality of porcine oocytes treated with $H_2O_2$.**

(**A**) Representative images of in vitro matured porcine oocytes in control, $H_2O_2$-treated, and Glu-supplemented groups. Scale bars, 120 μm, 120 μm, 30 μm. GV oocytes were treated with 100 μM $H_2O_2$ for 45 min and then cultured in the fresh medium with or without glutamic acid for in vitro maturation. (**B**) The rate of PB1 extrusion was recorded in control ($n = 216$), $H_2O_2$-treated ($n = 351$), and different concentrations of Glu-supplemented groups (50 μM: $n = 365$, 100 μM: $n = 339$; 200 μM: $n = 302$) after in vitro culture for 44 h. 200 μM Glu was used for subsequent analyses. ***$P = 0.0009$, ***$P = 0.0002$, ****$P < 0.0001$. (**C**) Representative images of spindle morphology and chromosome alignment in control, $H_2O_2$-treated, and Glu-supplemented oocytes. Scale bar, 5 μm. (**D**) The rate of abnormal spindles was measured in control ($n = 77$), $H_2O_2$-treated ($n = 75$), and Glu-supplemented ($n = 49$) oocytes. **$P = 0.0067$, *$P = 0.0340$. (**E**) The rate of misaligned chromosomes was measured in control ($n = 77$), $H_2O_2$-treated ($n = 75$), and Glu-supplemented ($n = 49$) oocytes. **$P = 0.0017$, *$P = 0.0395$. (**F**) Representative images of mitochondrial signals as shown by MitoTracker staining in control, $H_2O_2$-treated, and Glu-supplemented oocytes. Scale bar, 120 μm. (**G**) The fluorescence intensity of mitochondrial signals was measured in control ($n = 25$), $H_2O_2$-treated ($n = 24$), and Glu-supplemented ($n = 25$) oocytes. ****$P < 0.0001$, ****$P < 0.0001$. (**H**) Representative images of ROS levels as detected by DCFH-DA staining in control, $H_2O_2$-treated, and Glu-supplemented oocytes. Scale bar, 120 μm. (**I**) The fluorescence intensity of ROS signals was measured in control ($n = 38$), $H_2O_2$-treated ($n = 34$), and Glu-supplemented ($n = 21$) oocytes. **$P = 0.0033$, **$P = 0.0034$. Data in (**B**), (**D**), (**E**), (**G**), and (**I**) were presented as mean ± SEM or SD of at least three independent experiments. *$P < 0.05$; **$P < 0.01$; ***$P < 0.001$; ****$P < 0.0001$. Statistical significance was determined by two-tailed unpaired t-test.

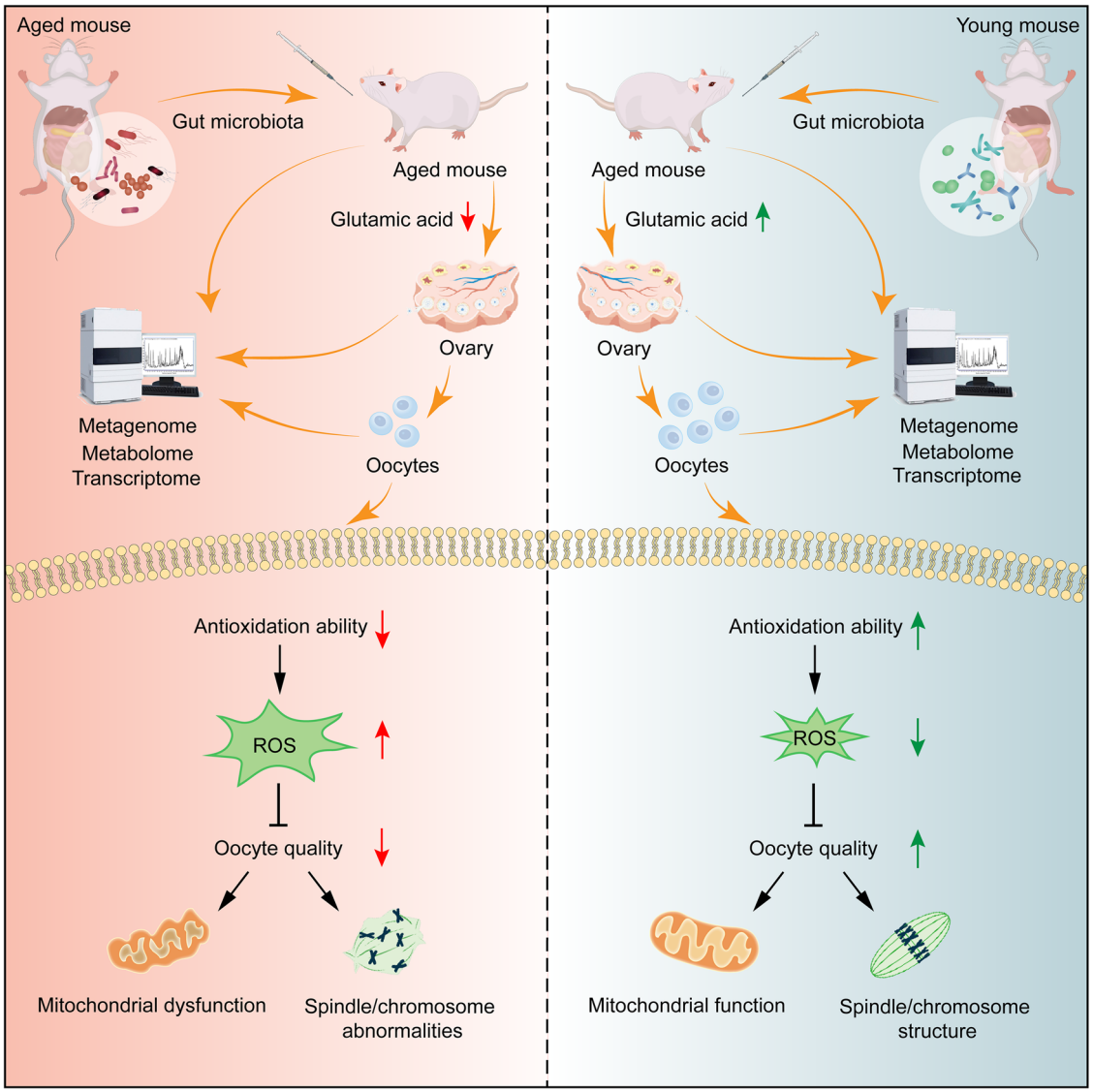


**Figure EV12.** Working model regarding how young gut microbiota rejuvenate the quality of maternally aged oocytes.